

# Probing primordial non-Gaussianity: The 3D Bispectrum of Ly- $\alpha$ forest and the redshifted 21-cm signal from the post reionization epoch

Tapomoy Guha Sarkar\*

Department of Physics, Birla Institute of Technology and Science,  
Pilani, Rajasthan, India.

Dhiraj Kumar Hazra<sup>†</sup>

Harish-Chandra Research Institute Chhatnag Road,  
Jhansi, Allahabad 211019, India

November 4, 2018

## Abstract

We explore possibility of using the three dimensional bispectra of the Ly- $\alpha$  forest and the redshifted 21-cm signal from the post-reionization epoch to constrain primordial non-Gaussianity. Both these fields map out the large scale distribution of neutral hydrogen and maybe treated as tracers of the underlying dark matter field. We first present the general formalism for the auto and cross bispectrum of two arbitrary three dimensional biased tracers and then apply it to the specific case. We have modeled the 3D Ly- $\alpha$  transmitted flux field as a continuous tracer sampled along 1D skewers which corresponds to quasars sight lines. For the post reionization 21-cm signal we have used a linear bias model. We use a Fisher matrix analysis to present the first prediction for bounds on  $f_{\text{NL}}$  and the other bias parameters using the three dimensional 21-cm bispectrum and other cross bispectra. The bounds on  $f_{\text{NL}}$  depend on the survey volume, and the various observational noises. We have considered a BOSS like Ly- $\alpha$  survey where the average number density of quasars  $\bar{n} = 10^{-3} \text{ Mpc}^{-2}$  and the spectra are measured at a  $2\text{-}\sigma$  level. For the 21-cm signal we have considered a 4000 hrs observation with a futuristic SKA like radio array. We find that bounds on  $f_{\text{NL}}$  obtained in our analysis ( $6 \leq \Delta f_{\text{NL}} \leq 65$ ) is competitive with CMBR and galaxy surveys and may prove to be an important alternative approach towards constraining primordial physics using future data sets. Further, we have presented a hierarchy of power of the bispectrum-estimators towards detecting the  $f_{\text{NL}}$ . Given the quality of the data sets, one may use this method to optimally choose the right estimator and thereby provide

---

\*tapomoy@bits-pilani.ac.in

<sup>†</sup>Current affiliation: Asia Pacific Center for Theoretical Physics, Pohang, Gyeongbuk 790-784, Korea.  
E-mail: dhiraj@apctp.org

better constraints on  $f_{\text{NL}}$ . We also find that by combining the various cross-bispectrum estimators it is possible to constrain  $f_{\text{NL}}$  at a level  $\Delta f_{\text{NL}} \sim 4.7$ . For the *equilateral* and *orthogonal* template we obtain  $\Delta f_{\text{NL}}^{\text{equ}} \sim 17$  and  $\Delta f_{\text{NL}}^{\text{orth}} \sim 13$  respectively for the combined estimator. This shall be important in the quest towards understanding the mechanism behind the generation of primordial perturbations.

## Contents

<b>1</b>	<b>Introduction</b>	<b>2</b>
<b>2</b>	<b>Formalism</b>	<b>3</b>
<b>3</b>	<b>Results and Discussion</b>	<b>8</b>
<b>4</b>	<b>Acknowledgements</b>	<b>13</b>

## 1 Introduction

In the study of inflationary cosmology, probing the deviations from Gaussian initial conditions offer valuable insights to our understanding of the mechanisms that generated primordial fluctuations. Whereas, departures from non-Gaussianity is very small for the standard single inflaton models [1], a wide class of theories predict a moderate to high non-Gaussianity [2]. Measuring the degree of primordial non-Gaussianity hence, directly allows us to narrow down the range of viable inflation models. The bispectrum or the three point correlation function of the density fluctuations is a standard quantifier of non-Gaussianity and the bispectrum of the CMBR temperature anisotropies and large scale structure have been extensively studied in this regard [3, 4, 5, 6]. Study of large scale structure using galaxy redshift surveys have also been proposed as means to constrain non-Gaussianity [7, 8]. A recent work has also proposed the use of three dimensional Ly- $\alpha$  forest to measure primordial non-Gaussianity [9]. The bispectrum of any good tracer of the underlying density field is, however a potential probe of primordial non-Gaussianity.

The neutral hydrogen (HI) distribution in the the post reionization IGM is a powerful cosmological probe of the low redshift universe. The complex astrophysical processes that dictate the HI distribution during the epoch of reionization, becomes largely irrelevant at redshifts  $z < 6$ . Here, two astrophysical systems are of observational interest. The dense and self shielded Damped Lyman  $\alpha$  (DLA) systems [10] house bulk of the HI and is the dominant source of the 21-cm signal [11](seen in emission). The HI density fluctuations in the predominantly ionized IGM, on the contrary is responsible for the distinct absorption features - the Ly- $\alpha$  forest [12], in the spectrum of back ground quasars. On large cosmological scales both the Ly- $\alpha$  forest and the redshifted 21-cm signal are believed to be biased tracers of the underlying dark matter distribution.

We note that the 21-cm signal from individual DLA clouds is extremely small. There, however maybe some enhancement due to gravitational lensing [13], but for most purposes it is reasonable to look at the large scale diffuse distribution of the signal which forms a

background in radio observations. This low resolution mapping of the 21-cm sky over large volumes at redshifts  $z < 3$  is called ‘Intensity Mapping’ [14, 15]. The large number density of DLAs make the Poisson noise arising from discrete sampling almost negligible [15].

The possibility of measuring the cross correlation power spectrum of the 21-cm signal and Ly- $\alpha$  forest has been proposed [16] as a means to bypass some of the observational issues. The two signals being tracers of the underlying large scale structure are expected to be correlated on large scales. However, foregrounds and other systematics are believed to be uncorrelated between the two independent observations. Hence, the cross correlation power spectrum signal if detected will clearly ascertain its cosmological origin. It is only natural to generalize the notion of cross power spectrum to cross-bispectrum of the two fields. The cross-bispectrum is an obvious byproduct of the two data sets that are used to measure the auto correlations. Further, an advantage of the cross-correlation study is that, in it, the demerits of one of the data sets gets partly compensated by the merits of the other.

The auto correlations of both the 21-cm maps [17] and the Ly- $\alpha$  forest [9] towards a measurement of primordial non-Gaussianity has been independently studied. In this paper we investigate the three dimensional cross-bispectrum of these cosmological fields. We set up the general formalism for calculating the cross-bispectrum of two arbitrary low redshift tracers of the underlying matter distribution. The general formalism is then applied to estimate the cross-bispectrum of 21-cm brightness temperature and Ly- $\alpha$  transmitted flux fields. We use a Fisher matrix analysis to investigate the possibility of constraining the non-Gaussianity parameter  $f_{\text{NL}}$  from the cross-bispectrum signal for a range of observational parameters. A comparison between the various auto and cross bispectra is also presented. We note that this is the first direct investigation of primordial non-Gaussianity using bispectrum of the entire three dimensional information contained in the distribution of low redshift neutral hydrogen.

## 2 Formalism

On sub-horizon scales the matter overdensity field  $\Delta_{\mathbf{k}}$  in Fourier space is related to the primordial gravitational potential as

$$\Delta_{\mathbf{k}}(z) = \mathcal{M}(k, z)\Phi_{\mathbf{k}}^{\text{prim}} = -\frac{3}{5}\frac{k^2 T(k)}{\Omega_m H_0^2} D_+(z)\Phi_{\mathbf{k}}^{\text{prim}}, \quad (1)$$

where  $T(k)$  denotes the matter transfer function and  $D_+(z)$  is the growing mode of density fluctuations. The statistical properties of  $\Delta_{\mathbf{k}}$  are quantified through the  $n$ -point correlations. The first two non-trivial of these are the power spectrum and bispectrum, defined respectively as

$$\begin{aligned} \langle \Delta_{\mathbf{k}_1} \Delta_{\mathbf{k}_2} \rangle &= \delta_D(\mathbf{k}_1 + \mathbf{k}_2) P(k_1) \\ \langle \Delta_{\mathbf{k}_1} \Delta_{\mathbf{k}_2} \Delta_{\mathbf{k}_3} \rangle &= \delta_D(\mathbf{k}_1 + \mathbf{k}_2 + \mathbf{k}_3) B(k_1, k_2, k_3). \end{aligned} \quad (2)$$

We assume that the primordial gravitational potential  $\Phi^{\text{prim}} = \phi_G$  may be written as

$$\Phi^{\text{prim}} = \phi_G + \frac{f_{\text{NL}}}{c^2} (\phi_G^2 - \langle \phi_G^2 \rangle), \quad (3)$$

where,  $\phi_G$  is a Gaussian random field and non-Gaussianity is quantified using a single parameter  $f_{\text{NL}}$ . The linear power spectrum of a sufficiently smoothed density field is given by

$$P^{\text{L}}(k) = \frac{9}{25} \frac{k^4 T^2(k)}{\Omega_m^2 H_0^4} D_+^2(z) P_{\Phi}^{\text{prim}}, \quad (4)$$

where  $P_{\Phi}^{\text{prim}}$  denotes the primordial power spectrum of the gravitational potential such that  $P_{\Phi}^{\text{prim}} = P_{\phi_G} + \mathcal{O}(f_{\text{NL}}^2)$ . The power spectrum  $P_{\phi_G}$  arising from the Gaussian field  $\phi_G$  does not exhibit exotic features and is scale invariant. In a linear theory the bispectrum arising from non-Gaussianity in the primordial matter field is given by

$$B_{123}^{\text{L}} = \mathcal{M}(k_1)\mathcal{M}(k_2)\mathcal{M}(k_3)B_{\phi_G 123}. \quad (5)$$

Here the notation  $123 \equiv (k_1, k_2, k_3)$  and we have used the form of  $B_{\phi_G 123}$  from earlier works [18, 9].

$$B_{\phi_G 123} = \frac{2f_{\text{NL}}}{c^2} [P_{\phi_G}(k_1)P_{\phi_G}(k_2) + \text{cyc}] + \mathcal{O}(f_{\text{NL}}^3). \quad (6)$$

Here we note that we are using the *local* template in the definition of  $f_{\text{NL}}$ . This choice of template makes the contribution to bispectrum predominantly coming from squeezed triangles. The *equilateral* and *orthogonal* templates upto linear order in  $f_{\text{NL}}$  are defined as [8, 19]

$$B_{\phi_G 123} = \frac{6f_{\text{NL}}^{\text{equ}}}{c^2} \left[ (-P_{\phi_G}(k_1)P_{\phi_G}(k_2) + 2 \text{cyc}) - \left( 2P_{\phi_G}(k_1)^{\frac{2}{3}}P_{\phi_G}(k_2)^{\frac{2}{3}}P_{\phi_G}(k_3)^{\frac{2}{3}} \right) + \left( P_{\phi_G}(k_1)^{\frac{1}{3}}P_{\phi_G}(k_2)^{\frac{2}{3}}P_{\phi_G}(k_3) + 5 \text{cyc} \right) \right]. \quad (7)$$

$$B_{\phi_G 123} = \frac{6f_{\text{NL}}^{\text{orth}}}{c^2} \left[ -(3P_{\phi_G}(k_1)P_{\phi_G}(k_2) + 2 \text{cyc}) - \left( 8P_{\phi_G}(k_1)^{\frac{2}{3}}P_{\phi_G}(k_2)^{\frac{2}{3}}P_{\phi_G}(k_3)^{\frac{2}{3}} \right) + \left( 3P_{\phi_G}(k_1)^{\frac{1}{3}}P_{\phi_G}(k_2)^{\frac{2}{3}}P_{\phi_G}(k_3) + 5 \text{cyc} \right) \right]. \quad (8)$$

Henceforth we shall use  $f_{\text{NL}}$  without any superscript to denote the *local* template.

The measurement of  $n$ -point functions of the matter density field is usually implicit. One actually measures the statistical properties of the low redshift biased tracers. At lower redshifts one needs to incorporate non-linear structure formation caused by gravitational instability. This induces additional non-Gaussianity in addition to the contribution from primordial sources. The additional contribution to the matter bispectrum,  $B_{123}^{\text{NL}}$  [18, 9] is obtained from the second order perturbation theory. Hence,

$$B_{123}^{\text{NL}} = 2F_2(\mathbf{k}_1, \mathbf{k}_2)P(k_1)P(k_2) + \text{cyc}, \quad (9)$$

where  $F_2(\mathbf{k}_1, \mathbf{k}_2)$ , adopted from [18] is given by

$$F_2(\mathbf{k}_1, \mathbf{k}_2) = \frac{5}{7} + \frac{\hat{k}_1 \cdot \hat{k}_2}{2} \left( \frac{k_1}{k_2} + \frac{k_2}{k_1} \right) + \frac{2}{7} (\hat{k}_1 \cdot \hat{k}_2)^2. \quad (10)$$

The total matter bispectrum is hence given by the sum

$$B_{123} = B_{123}^L + B_{123}^{\text{NL}}, \quad (11)$$

where a possible contribution from the primordial trispectrum has been ignored.

Let us consider tracer fields denoted by  $R$  and  $S$  which are related to the underlying matter overdensity field as

$$R(\mathbf{k}) [S(\mathbf{k})] = b_{R[S]}^{(1)} \Delta(\mathbf{k}) + \frac{b_{R[S]}^{(2)}}{2} \Delta(\mathbf{k})^2. \quad (12)$$

We are interested in the statistical properties of these tracers. The cross-correlation power spectrum  $P_{RS}$  for the tracer fields and bispectra  $\mathcal{B}_{RRS}$ , in the leading order are related to the matter power spectrum and the bispectrum as,

$$\begin{aligned} P_{RS}(k) &= b_R^{(1)} b_S^{(1)} P(k) \\ \mathcal{B}_{RSS}(k_1, k_2, k_3) &= \frac{b_R^{(1)} b_S^{(1)2}}{3} [B_{123} + B_{231} + B_{312}] + \frac{1}{3} \left[ 2b_R^{(1)} b_S^{(1)} b_S^{(2)} (P(k_1)P(k_2) + \text{cyc.}) \right. \\ &\quad \left. + b_R^{(2)} b_S^{(1)} b_S^{(1)} (P(k_1)P(k_2) + \text{cyc.}) \right]. \end{aligned} \quad (13)$$

We note that for  $R = S$  we have the auto-correlation power spectrum and bispectrum. Following the formalism in [18] we define the generalized bispectra estimators  $\hat{\mathcal{B}}_\epsilon$  with  $\epsilon = R, RSS$  as

$$\hat{\mathcal{B}}_\epsilon = \frac{V_f}{V_{123}} \int_{k_1} d^3 \mathbf{q}_1 \int_{k_2} d^3 \mathbf{q}_2 \int_{k_3} d^3 \mathbf{q}_3 \delta_D(\mathbf{q}_{123}) \times \Pi_\epsilon(k_1, k_2, k_3). \quad (14)$$

Here  $\mathbf{q}_{123} = \mathbf{q}_1 + \mathbf{q}_2 + \mathbf{q}_3$ ,  $V_f = (2\pi)^3/V$  where  $V$  is the survey volume, and  $V_{123}$  is given by,

$$V_{123} = \int_{k_1} d^3 \mathbf{q}_1 \int_{k_2} d^3 \mathbf{q}_2 \int_{k_3} d^3 \mathbf{q}_3 \delta_D(\mathbf{q}_{123}), \quad (15)$$

and the integrals are performed over the  $q_i$ - intervals  $(k_i - \frac{\delta k}{2}, k_i + \frac{\delta k}{2})$ . The integrands are given by  $\Pi_{RSS} = (1/3)[\Delta_R^o(k_1)\Delta_S^o(k_2)\Delta_S^o(k_3) + \text{cyc.}]$ . The ‘observed’ fields  $\Delta_S^o(k_i)$  or  $\Delta_R^o(k_i)$  in Fourier space contain noise contributions and are in general different from the respective cosmological fields  $\Delta_S(k_i)$  and  $\Delta_R(k_i)$ . The estimators defined above are unbiased and their variances can be calculated using the relation  $\Delta \hat{\mathcal{B}}_\epsilon^2 = \langle \hat{\mathcal{B}}_\epsilon^2 \rangle - \langle \hat{\mathcal{B}}_\epsilon \rangle^2$ . In the leading order this yields the following

$$\begin{aligned} \Delta \hat{\mathcal{B}}_{RSS}^2(k_1, k_2, k_3) &= \frac{V_f}{9V_{123}} [t (P_R^{\text{Tot}}(k_1)P_S^{\text{Tot}}(k_2)P_S^{\text{Tot}}(k_3) + \text{cyc.}) \\ &\quad + 2t (P_S^{\text{Tot}}(k_1)P_{RS}^{\text{Tot}}(k_2)P_{RS}^{\text{Tot}}(k_3) + \text{cyc.})]. \end{aligned} \quad (16)$$

As earlier,  $R = S$  gives the variance for the auto correlation bispectrum. The combinatorial factor  $t = 6, 1$  for equilateral and scalene triangles respectively and  $P^{\text{Tot}}$  includes any additional noise power spectra along with the cosmological power spectrum. Armed with the results in equation (13) and equation (16), we shall apply the general formalism to the two

tracer fields of interest namely the Ly- $\alpha$  forest spectra and redshifted 21-cm signal, both of which are related to the neutral hydrogen distribution.

Observations indicate that, following the epoch of reionization, bulk of the neutral gas is contained in the self shielded DLA systems [10]. The collective 21-cm emission from these clouds is known to form a diffused background in low frequency radio observations. We use  $\delta_T$  to denote the fluctuations in the brightness temperature of redshifted 21-cm radiation. We are interested in the redshift range  $z < 3.5$  whereby it is reasonable to assume that  $\delta_T$  is a biased tracer of the underlying dark matter distribution. The numerical simulations of the post reionization 21 -cm signal [20, 21], show that a constant scale independent bias model is adequate to describe the large scale distribution of the 21-cm signal at the relevant redshifts.

The transmitted flux  $\mathcal{F}$  through the Ly- $\alpha$  forest may be modeled by assuming that the gas traces the underlying dark matter distribution [23] except on small scales where pressure plays an important role. Further, it is believed that photo-ionization equilibrium that maintains the neutral fraction, also leads to a power law temperature-density relation [24]. On large scales it is reasonable to assume that the fluctuations in the transmitted flux  $\delta_{\mathcal{F}} = (\mathcal{F}/\bar{\mathcal{F}} - 1)$  traces the dark matter field, with the implicit assumption that the Ly- $\alpha$  forest spectrum has been smoothed over some suitably large length scale.

With all the assumptions discussed above we may relate fluctuations in Fourier space for both the 21-cm temperature and Ly- $\alpha$  transmitted flux to the dark matter fluctuations as in equation (12). Note, that this model depends on 4 parameters ( $b_T^{(1)}, b_T^{(2)}, b_{\mathcal{F}}^{(1)}, b_{\mathcal{F}}^{(2)}$ ) apart from the large scale dark matter distribution and the underlying cosmological model. For the 21-cm brightness temperature field we have (for the WMAP7 cosmological parameters)  $b_T^{(1)} = 4.0 \text{ mK } b_{21} \bar{x}_{\text{HI}} (1+z)^2 H_0/H(z)$ , where  $\bar{x}_{\text{HI}}$  is the mean neutral fraction. The neutral hydrogen fraction is believed to be a constant with a value  $\bar{x}_{\text{HI}} = 2.45 \times 10^{-2}$  using  $\Omega_{\text{gas}} \sim 10^{-3}$  [25]. The quantity  $b_{21}(k, z)$  is studied in numerical simulations [20, 21]. We adopt a constant bias  $b_{21} = 2$  at our fiducial redshift  $z = 2.5$  from these simulation results. For the Ly- $\alpha$  forest, we use an approximate  $b_{\mathcal{F}}^{(1)} \approx -0.13$  from the numerical simulations of Ly- $\alpha$  forest [22]. We note however that these numbers suffer from large uncertainties owing to our lack of a complete model of the IGM.

A Ly- $\alpha$  survey usually covers a large volume, as compared to a single field of view redshifted 21-cm observation. The cross-correlation can however be computed only in the region of overlap between the two fields.

For the Ly- $\alpha$  forest flux measurements the observed flux fluctuations in Fourier space is given by

$$\Delta_{\mathcal{F}}^o(\mathbf{k}) = \tilde{\rho}(\mathbf{k}) \otimes \Delta_{\mathcal{F}}(\mathbf{k}) + \Delta_{\mathcal{F}\text{noise}}(\mathbf{k}), \quad (17)$$

where  $\tilde{\rho}$  is the sampling window function in Fourier space, and  $\Delta_{\mathcal{F}\text{noise}}(\mathbf{k})$  denotes a possible noise term. The function takes care of the discrete sampling of the skewers corresponding to the quasar lines of sight. In the variance calculation using equation (16) we use  $P_{\mathcal{F}}^{\text{Tot}}(k)$  as the total power spectrum of Ly- $\alpha$  flux given by [26]

$$P_{\mathcal{F}}^{\text{Tot}}(\mathbf{k}) = P_{\mathcal{F}}(\mathbf{k}) + P_{\mathcal{F}}^{\text{1D}}(k_{\parallel})P_W + N_{\mathcal{F}}, \quad (18)$$

where  $P_{\mathcal{F}}(\mathbf{k}) = b_{\mathcal{F}}^{(1)2} P(\mathbf{k})$ , the quantity  $P_{\mathcal{F}}^{\text{1D}}(k_{\parallel})$  is the usual 1D flux power spectrum [23]

corresponding to individual spectra given by

$$P_{\mathcal{F}}^{\text{1D}}(k_{\parallel}) = (2\pi)^{-2} \int d^2\mathbf{k}_{\perp} P_{\mathcal{F}}(\mathbf{k}) \quad (19)$$

and  $P_W$  denotes the power spectrum of the window function. The quantity  $N_{\mathcal{F}}$  denotes the effective noise power spectra for the Ly- $\alpha$  observations. The ‘aliasing’ term  $P_{\mathcal{F}}^{\text{1D}}(k_{\parallel})P_W$  quantifies the discreteness of the 1D Ly- $\alpha$  skewers. If the Ly- $\alpha$  spectra are measured with a sufficiently high SNR, it maybe shown that each quasar line of sight may actually be given the same weight and  $P_W = \frac{1}{\bar{n}}$ , where  $\bar{n}$  is the 2D density of quasars ( $\bar{n} = N_Q/\mathcal{A}$ , where  $\mathcal{A}$  is the area of the observed field of view) [27]. We assume that the variance  $\sigma_{\mathcal{F}N}^2$  of the pixel noise contribution to  $\delta_{\mathcal{F}}$  is the same across all the quasar spectra. It is related to the signal to noise ratio on the continuum and depends on the size of the pixel. Hence we have  $N_{\mathcal{F}} = \sigma_{\mathcal{F}N}^2/\bar{n}$  for its the noise power spectrum.

$$N_{\mathcal{F}} = \frac{1}{\bar{n}} \langle \bar{\mathcal{F}} \rangle^{-2} [S/N]_{\Delta x}^{-2} (\Delta x/1 \text{ Mpc}). \quad (20)$$

We shall henceforth refer to this noise for  $S/N$  in  $1\text{Å}$  pixels. In arriving at equation (18) the effect of quasar clustering [28] has been ignored with the assumption that dominant contribution to noise comes from the Poisson term for Quasar surveys with realistic values of  $\bar{n}$ .

For the 21-cm observations one may ignore the discrete nature of the DLA sources. We consider a radio-interferometric measurement of the redshifted 21-cm signal with the total signal is given by

$$P_{\text{T}}^{\text{Tot}} = P_{\text{T}}(\mathbf{k}) + N_{\text{T}}. \quad (21)$$

The cosmological component of the signal is  $P_{\text{T}}(\mathbf{k}) = (b_{\text{T}}^{(1)})^2 P(\mathbf{k})$  and the noise power spectrum [29]  $N_{\text{T}}$  at an observed frequency  $\nu = 1420/(1+z)\text{MHz}$  can be calculated using the relation

$$N_{\text{T}}(k, \nu) = \frac{T_{\text{sys}}^2}{Bt_0} \left( \frac{\lambda^2}{A_e} \right)^2 \frac{r_{\nu}^2 l}{n_b(U, \nu)}. \quad (22)$$

Here  $T_{\text{sys}}$  denotes the sky dominated system temperature,  $B$  is the observation bandwidth,  $t_0$  is the total observation time,  $r_{\nu}$  is the comoving distance to the redshift  $z$ ,  $l$  is the comoving length corresponding to the bandwidth  $B$ ,  $n_b(U, \nu)$  is the number density of baseline  $U$ , where  $U = k_{\perp} r_{\nu}/2\pi$ , and  $A_e$  is the effective collecting area for each individual antenna. We may write  $n_b(U, \nu) = N(N-1)f_{2D}(U, \nu)/2$  where  $N$  is the total number of antenna in the radio array and  $f_{2D}(U, \nu)$  is the normalized baseline distribution function [30, 31].

We use a Fisher matrix analysis to constrain  $f_{\text{NL}}$  from the observables of relevance here, namely the auto and cross bispectra  $\mathcal{B}$  (the index  $\epsilon$  is dropped for brevity). The Fisher matrix for a set of model parameters  $p_i$  is given by

$$F_{ij} = \sum_{\text{RS}} \sum_{k_1=k_{\min}}^{k_{\max}} \sum_{k_2=k_{\min}}^{k_1} \sum_{k_3=\tilde{k}_{\min}}^{k_2} \frac{1}{\Delta \mathcal{B}_{\text{RSS}}^2} \frac{\partial \mathcal{B}_{\text{RSS}}}{\partial p_i} \frac{\partial \mathcal{B}_{\text{RSS}}}{\partial p_j}, \quad (23)$$

where  $\tilde{k}_{\min} = \mathbf{max}(k_{\min}, |k_1 - k_2|)$  and the summations are performed using  $\delta k = k_{\min}$ . Assuming that the likelihood functions for  $p_i$  are Gaussian distributed, the corresponding



minimum errors in  $p_i$  are limited by the Cramer-Rao bound  $\sigma_i^2 = F_{ii}^{-1}$ . We have modeled the Ly- $\alpha$  and 21-cm signals using a set of bias parameters and the non-Gaussianity parameter so that  $p_i = (f_{\text{NL}}, b_{\text{T}}^{(1)}, b_{\text{T}}^{(2)}, b_{\mathcal{F}}^{(1)}, b_{\mathcal{F}}^{(2)})$ . We shall use the Fisher matrix to investigate the power of a Ly- $\alpha$  survey and 21-cm observation to constrain these parameters.

### 3 Results and Discussion

We consider a radio interferometric observation of the redshifted 21-cm signal at a fiducial redshift  $z = 2.5$ . The choice of redshift is justified by a priori knowledge of quasar distribution which is known to peak between  $z = 2$  and  $z = 3$ . We consider a futuristic radio observation with a SKA<sup>1</sup> like radio array with 1400 antennas, each offering an effective area of 45 m<sup>2</sup> (fov  $\sim \pi 8.6^2 \text{deg}^2$ ), spread out with an approximately uniform baseline distribution. The observing central frequency is taken to be 406 MHz corresponding to  $z = 2.5$ . The system temperature is dominated by the sky temperature and is assumed to be of the form  $T_{\text{sys}} = \left[ 60 \left[ \frac{1+z}{4.73} \right]^{2.55} + 50 \right]$  K [32]. The noise estimates depend crucially on the volume of the survey. We take  $k_{\text{min}} = 0.012 \text{ Mpc}^{-1}$  and  $k_{\text{max}} = 0.2 \text{ Mpc}^{-1}$  for a single field of view observation and consider a total observing time of 4000 hrs.

Typically, the Ly- $\alpha$  surveys have a much larger sky coverage in the transverse direction than single field radio observations. In the radial direction, the frequency bandwidth of radio telescope dictates the volume of the 21-cm survey. For the Ly- $\alpha$  forest observations parts of the spectra contaminated by Ly- $\beta$  or O – VI lines at one end and quasar proximity effect on the other end, may not be used and the correlation can be measured in a smaller redshift interval. The cross-correlation can however only be measured in the overlapping regions. We have considered a Ly- $\alpha$  spectroscopic survey with  $\bar{n} = 10^{-3} \text{ Mpc}^{-2}$  which is assumed to be constant across the redshift range of interest. We note that  $\bar{n}$  shall in general be dependent on the central redshift and magnitude limit of the survey. We also assume that the spectra are measured with a S/N = 2 for 1 $\text{\AA}$  pixels. We consider a BOSS<sup>2</sup> like survey which gives us  $k_{\text{min}} = 2 \times 10^{-3} \text{ Mpc}^{-1}$  and  $k_{\text{max}} = 1 \text{ Mpc}^{-1}$  respectively. The cross-bispectrum between the 21-cm signal and Ly- $\alpha$  forest may either include two Ly- $\alpha$  component and one 21-cm component or vice-versa. We denote these as  $\mathcal{B}_{\mathcal{F}\mathcal{F}\text{T}}$  and  $\mathcal{B}_{\text{T}\text{T}\mathcal{F}}$  respectively. Both of these can be estimated from the same data sets. However, the relative merits depends on the nature of the observations and quality of the data.

The cross correlation may be computed in the volume spanned by the 21-cm observation, which is smaller than the coverage of the Ly- $\alpha$  survey. Further, the signal with higher resolution (in this case Ly- $\alpha$  forest) has to be smoothed to match the poorer resolution of the other field. The bispectra are then obtained for arbitrary triangles assuming that the primordial power spectrum is generated by a quadratic inflaton potential and the background cosmological parameters are frozen to their best fit values from WMAP7 year data [33].

We first consider  $\mathcal{B}_{\mathcal{F}\text{T}\text{T}}$ . The Fisher matrix analysis is used to obtain bounds on the parameters  $(f_{\text{NL}}, b_{\text{T}}^{(1)}, b_{\mathcal{F}}^{(1)})$ . The Likelihood function is assumed to be a Gaussian, which yields the confidence ellipses in the parameter space centered at the fiducial values of the

---

<sup>1</sup><http://www.skatelescope.org>

<sup>2</sup><http://cosmology.lbl.gov/BOSS/>



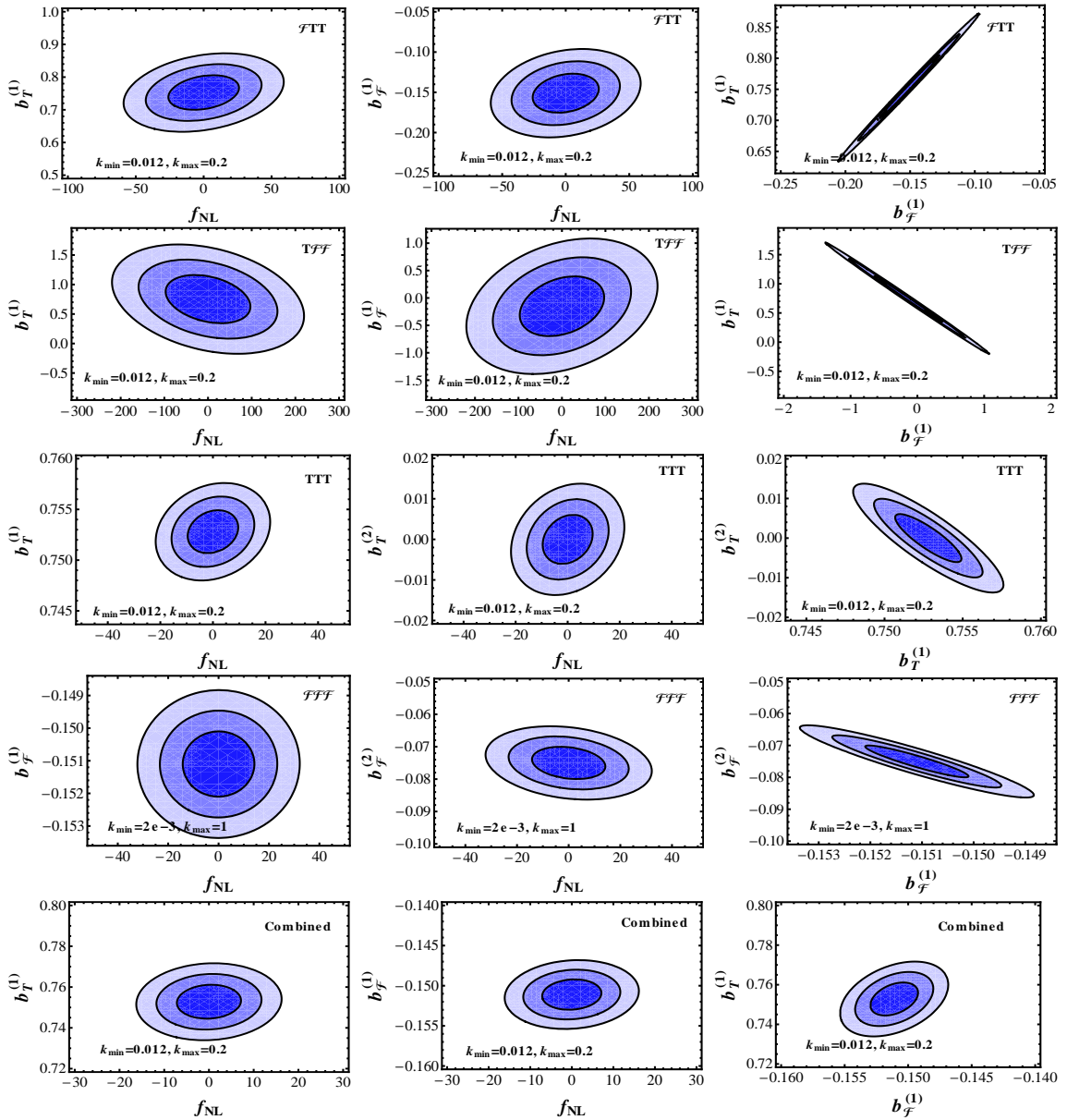


Figure 1: The 68.3%, 95.4% and 99.8% likelihood confidence contours for  $f_{\text{NL}}$  and various bias parameters. Shown in the figure are the values  $k_{\text{min}}$  and  $k_{\text{max}}$  (unit  $\text{Mpc}^{-1}$ ) used to compute the Fisher matrix for different estimators mentioned in the plots. The bispectrum estimators used for analysis are  $\mathcal{FTT}$ ,  $\mathcal{TFF}$ ,  $\mathcal{TTT}$ ,  $\mathcal{FFF}$ . The lowest panel shows the confidence ellipses for the combined estimator.

corresponding parameters. Figure 1 (top panel) shows these results for  $\mathcal{B}_{\mathcal{FTT}}$ . The tilt of the ellipse measures the correlation between the parameters, and the semi major/minor axes measures the maximum uncertainties in measurement of the parameters. The correlation between parameters  $p_i$  and  $p_j$  is measured using a coefficient  $r_{ij} = F_{ij}^{-1} / \sqrt{F_{ii}^{-1} F_{jj}^{-1}}$ . The

strong correlation between  $b_T^{(1)}$  and  $b_F^{(1)}$  ( $r \sim 0.997$ ) reflects the fact that these parameters occur as a product in the cross-powerspectra. We find that it is possible to constrain  $f_{\text{NL}}$  at a level  $\Delta f_{\text{NL}} = 17$  for the given observational parameters. When we consider  $\mathcal{B}_{\text{TFF}}$  (see Figure (1)) the bounds on  $f_{\text{NL}}$  worsens and we have  $\Delta f_{\text{NL}} = 64$ . This is because - as compared to  $\mathcal{B}_{\text{TFF}}$  the quantity  $\mathcal{B}_{\text{FTT}}$  has a greater dependence on the 21 cm signal which appears twice in it and the SKA parameters chosen here makes the 21-cm signal less noisy as compared to the  $2-\sigma$  Ly- $\alpha$  spectra. The situation would be reversed if the Ly- $\alpha$  forest had high SNR and the 21-cm observation was relatively more noisy. The numerical results are summarized in the table (1). For the cross bispectra, the volume of the overlap region dictates the sensitivity. Between the two fields being used to compute the bispectrum, the one which appears twice should have higher SNR, to yield better constraints on the parameters.

For the auto bispectra, the survey volume and the observational noise decides the errors on the parameters being estimated. For the 21-cm signal and Ly- $\alpha$  forest auto correlation we choose the parameters  $(f_{\text{NL}}, b_T^{(1)}, b_T^{(2)})$  and  $(f_{\text{NL}}, b_F^{(1)}, b_F^{(2)})$  respectively. We use the fiducial values  $b_T^{(2)} = b_F^{(2)} = 0$  in our Fisher analysis. For the Ly- $\alpha$  forest, the SNR for the individual spectra is low. This is compensated by the large survey volume. With the given noise parameters, the constraint on  $f_{\text{NL}}$  from the 21-cm and Ly- $\alpha$  bispectrum are of the same order with bounds  $\Delta f_{\text{NL}} = 9.4$  obtained from  $\mathcal{B}_{\text{FFF}}$  and  $\Delta f_{\text{NL}} = 6.3$  obtained from  $\mathcal{B}_{\text{TTT}}$ . A strong correlation between the linear and quadratic bias parameters is also seen in both the cases (see Figure (1) lower two panels). We note here that this is the first prediction of constraints on  $f_{\text{NL}}$  from 21-cm signal and Ly- $\alpha$  forest using the three dimensional analysis with the Bispectrum estimator for arbitrary triangular configurations.

It may appear from the above analysis that a certain combination of  $\mathcal{F}$  and  $\mathcal{T}$  has a greater

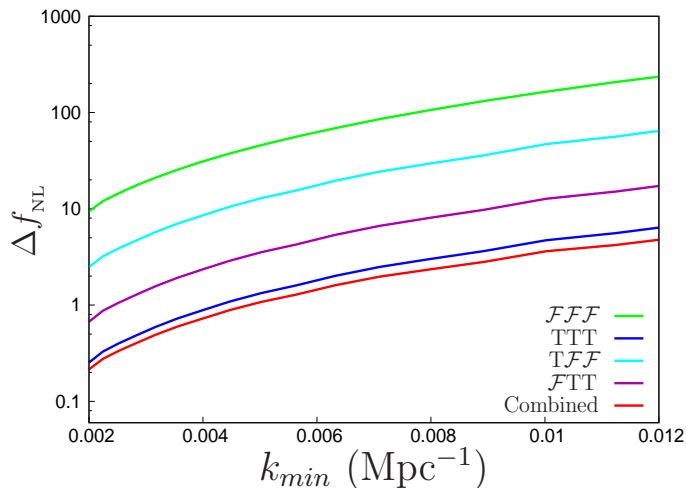


Figure 2: The bounds on  $f_{\text{NL}}$  for different estimators as a function of  $k_{\text{min}}$  assuming same SNR and observation time. Clearly this plot indicates a hierarchy of power to constrain  $f_{\text{NL}}$  between different estimators. However, this hierarchy is specific to the observational parameters and noise levels associated with the two fields.

advantage over the others. This hierarchy arises from the individual noise levels for the respective observations. One may however combine the information contained in all the

Estimator	$\mathcal{F}\mathcal{F}\mathcal{F}$	$\mathcal{T}\mathcal{F}\mathcal{F}$	$\mathcal{F}\mathcal{T}\mathcal{T}$	$\mathcal{T}\mathcal{T}\mathcal{T}$	Combined
Parameters	$p_2 = b_{\mathcal{F}}^{(1)}$ $p_3 = b_{\mathcal{F}}^{(2)}$	$p_2 = b_{\mathcal{T}}^{(1)}$ $p_3 = b_{\mathcal{F}}^{(1)}$	$p_2 = b_{\mathcal{T}}^{(1)}$ $p_3 = b_{\mathcal{F}}^{(1)}$	$p_2 = b_{\mathcal{T}}^{(1)}$ $p_3 = b_{\mathcal{T}}^{(2)}$	$p_2 = b_{\mathcal{T}}^{(1)}$ $p_3 = b_{\mathcal{F}}^{(1)}$
$\Delta f_{\text{NL}}$	9.4	64	17.2	6.3	4.7
$\Delta p_2$	$7 \times 10^{-4}$	0.28	$3.5 \times 10^{-2}$	$1.4 \times 10^{-3}$	$5.5 \times 10^{-3}$
$\Delta p_3$	$3 \times 10^{-3}$	0.36	$2 \times 10^{-2}$	$4 \times 10^{-3}$	$1.2 \times 10^{-3}$
$r_{12}$	$4 \times 10^{-3}$	-0.31	0.27	0.2	$7 \times 10^{-2}$
$r_{13}$	-0.21	0.3	0.21	0.22	0.1
$r_{23}$	-0.93	-0.99	0.99	-0.86	0.4

Table 1: The bounds on various parameters and their correlations obtained from Fisher analysis for different bispectrum estimators. Note that the parameter  $p_1$  denotes  $f_{\text{NL}}$  in all the estimators.

individual estimators to increase the SNR to a maximum for a given set of observational parameters. We have performed the full Fisher analysis using all the 5 parameters and including all the possible combinations of  $\mathcal{F}$  and  $\mathcal{T}$ . However, the  $k$ -range chosen for this analysis is taken to be corresponding to the common coverage and resolution of the two surveys. This, as expected yields the best SNR and a bound on  $\Delta f_{\text{NL}} \sim 4.7$ . Tighter constraints on the bias parameters are also obtained in the combined analysis (see table (1)).

Table (2) and table (3) shows the results obtained for the *equilateral* and *orthogonal* templates respectively. The degradation of the bounds obtained is on expected lines and we have  $\Delta f_{\text{NL}}^{\text{equ}} = 16.8$  and  $\Delta f_{\text{NL}}^{\text{orth}} = 13$  for the combined estimator.

As noted earlier, the volume of the survey plays a crucial role in the estimation of the parameters. It fixes the largest scales  $k_{\text{min}}$  that one may probe. Figure 2 shows the variation of the error on  $f_{\text{NL}}$  with  $k_{\text{min}}$  for a given set of experimental parameters. It indicates that, for all the bispectra estimators considered, there is a monotonic increase of  $\Delta f_{\text{NL}}$  with  $k_{\text{min}}$ . The constraints on  $f_{\text{NL}}$  hence, gets worse when  $k_{\text{min}}$  is increased. This is expected, since increasing  $k_{\text{min}}$  leads to the availability of lesser number of  $k$ -modes.

In our analysis, the observational parameters have been kept constant throughout. In reality the relative merit or demerit of a given estimator will depend on the noise in the data sets. The complete exploration of the full range of observational parameters for the two fields is required to be done to judge which estimator yields tighter constraint on  $f_{\text{NL}}$  as compared to the others and for what values of the observational parameters can that be achieved.

Estimator	$\mathcal{FFF}$	$\mathcal{TFF}$	$\mathcal{FTT}$	$\mathcal{TTT}$	Combined
Parameters	$p_2 = b_{\mathcal{F}}^{(1)}$ $p_3 = b_{\mathcal{F}}^{(2)}$	$p_2 = b_{\mathcal{T}}^{(1)}$ $p_3 = b_{\mathcal{F}}^{(1)}$	$p_2 = b_{\mathcal{T}}^{(1)}$ $p_3 = b_{\mathcal{F}}^{(1)}$	$p_2 = b_{\mathcal{T}}^{(1)}$ $p_3 = b_{\mathcal{T}}^{(2)}$	$p_2 = b_{\mathcal{T}}^{(1)}$ $p_3 = b_{\mathcal{F}}^{(1)}$
$\Delta f_{\text{NL}}^{\text{equ}}$	62	209	77	37	16.8
$\Delta p_2$	$8.2 \times 10^{-4}$	0.40	$6.09 \times 10^{-2}$	$1.8 \times 10^{-2}$	$5.7 \times 10^{-3}$
$\Delta p_3$	$4.6 \times 10^{-3}$	0.51	$2.73 \times 10^{-2}$	$8 \times 10^{-2}$	$1.3 \times 10^{-3}$
$r_{12}$	0.58	-0.74	0.83	-0.69	-0.26
$r_{13}$	-0.71	0.73	0.81	0.88	-0.38
$r_{23}$	-0.95	-0.99	0.99	-0.93	0.44

Table 2: The bounds on various parameters and their correlations obtained for the *equilateral* template

Estimator	$\mathcal{FFF}$	$\mathcal{TFF}$	$\mathcal{FTT}$	$\mathcal{TTT}$	Combined
Parameters	$p_2 = b_{\mathcal{F}}^{(1)}$ $p_3 = b_{\mathcal{F}}^{(2)}$	$p_2 = b_{\mathcal{T}}^{(1)}$ $p_3 = b_{\mathcal{F}}^{(1)}$	$p_2 = b_{\mathcal{T}}^{(1)}$ $p_3 = b_{\mathcal{F}}^{(1)}$	$p_2 = b_{\mathcal{T}}^{(1)}$ $p_3 = b_{\mathcal{T}}^{(2)}$	$p_2 = b_{\mathcal{T}}^{(1)}$ $p_3 = b_{\mathcal{F}}^{(1)}$
$\Delta f_{\text{NL}}^{\text{orth}}$	31	143	44	17.6	13
$\Delta p_2$	$7.8 \times 10^{-4}$	0.37	$5.11 \times 10^{-2}$	$2.2 \times 10^{-3}$	$6.3 \times 10^{-3}$
$\Delta p_3$	$3.5 \times 10^{-3}$	0.48	$2.41 \times 10^{-2}$	$6.1 \times 10^{-3}$	$1.6 \times 10^{-3}$
$r_{12}$	0.51	-0.68	0.74	-0.8	-0.49
$r_{13}$	-0.38	0.69	0.75	0.79	-0.64
$r_{23}$	-0.95	-0.99	0.99	-0.98	0.57

Table 3: The bounds on various parameters and their correlations obtained for the *orthogonal* template.

The predictions made in our analysis are optimistic and shall undergo some degradation with the inclusion of more realistic and complete noise or foreground. However, the present analysis indicates that our constraints on  $f_{\text{NL}}$  are much better than the SDSS ( $\Delta f_{\text{NL}} \sim 255$  and  $\Delta f_{\text{NL}}^{\text{equ}} \sim 1775$ ) and is competitive or better than the predictions for the CIP<sup>3</sup> survey ( $\Delta f_{\text{NL}} \sim 4.7$  and  $\Delta f_{\text{NL}}^{\text{equ}} \sim 51$ . See table 1. in [8]).

Several observational issues pose severe hindrance towards detecting the cosmological signals. For the 21-cm signal, astrophysical foregrounds which are several order higher than the signal completely submerge the cosmological information [34]. Several methods using the distinct spectral behavior of the foregrounds as compared to the signal has been proposed to clean the observed maps and retrieve the cosmological signal [35]. In this work we have assumed that for the 21-cm field, foreground cleaning has been done. For the Ly- $\alpha$  forest, a host of issues need to be addressed. This includes a proper modeling and subtraction of the continuum, tackling of contamination from metal lines in the forest [36], effect of Galactic super winds, to mention just a few. Redshift space distortion plays a crucial role on scales of our interest and is required to be incorporated in our analysis. We intend to take this up along with a detailed analysis of observational aspects and instrumental noise in a future work.

We conclude by noting that the three dimensional distribution of the post-reionization neutral hydrogen as probed using the 21-cm or the Ly- $\alpha$  forest, may be potentially used to estimate various auto/cross bispectra and thereby enrich our understanding of the early Universe.

## 4 Acknowledgements

D.K.H wishes to acknowledge support from the Korea Ministry of Education, Science and Technology, Gyeongsangbuk-Do and Pohang City for Independent Junior Research Groups at the Asia Pacific Center for Theoretical Physics.

## References

- [1] J. Maldacena, JHEP **0305**, 013 (2003); D. K. Hazra, L. Sriramkumar and J. Martin, [arXiv:1201.0926v2](https://arxiv.org/abs/1201.0926v2) [astro-ph.CO]
- [2] N. Bartolo, E. Komatsu, S. Matarrese and A. Riotto, Phys. Rept. **402**, 103 (2004).
- [3] D. Larson *et al.*, Astrophys. J. Suppl. **192**, 16 (2011);
- [4] E. Komatsu *et al.*, Astrophys. J. Suppl. **192**, 18 (2011);
- [5] K. M. Smith, L. Senatore and M. Zaldarriaga, JCAP **0909**, 006 (2009)
- [6] F. De Bernardis, P. Serra, A. Cooray and A. Melchiorri, Phys. Rev. D **82**, 083511 (2010).
- [7] R. Scoccimarro, E. Sefusatti and M. Zaldarriaga, Phys. Rev. D **69**, 103513 (2004).

---

<sup>3</sup><http://www.cfa.harvard.edu/cip/>

- [8] E., Sefusatti and E. Komatsu, Phys. Rev. D, **76**, 083004 (2007)
- [9] D. K. Hazra and T. Guha Sarkar, Phys. Rev. Lett. **109**, 121301 (2012).
- [10] A. M. Wolfe, E. Gawiser and J. X. Prochaska, Ann. Rev. Astron. Astrophys. **43**, 861 (2005).
- [11] S. Furlanetto, S. P. Oh and F. Briggs, Phys. Rept. **433**, 181 (2006).
- [12] M. Rauch, Ann. Rev. Astron. Astrophys. **36**, 267 (1998).
- [13] T. D. Saini, S. Bharadwaj and S. K. Sethi, Astrophys. J. **557** , 421 (2001)
- [14] T.-C. Chang, U.-L. Pen, J. B. Peterson and P. McDonald, Physical Review Letters, **100**, 091303 (2008)
- [15] S. Wyithe and A. Loeb, MNRAS **383**, 606 (2008)
- [16] T. Guha Sarkar, S. Bharadwaj, T. R. Choudhury, and K. K. Datta, Mon. Not. Roy. Astron. Soc., **410**, 1130 (2011).
- [17] S. Joudaki, O. Dore, L. Ferramacho, M. Kaplinghat and M. G. Santos, Phys. Rev. Lett. **107**, 131304 (2011).
- [18] V. Desjacques and U. Seljak, Class. Quant. Grav. **27**, 124011 (2010);
- [19] R. Scoccimarro, L. Hui, M. Manera and K. C. Chan, Phys. Rev. D, **85**, 083002 (2012)
- [20] N. Khandai, K. K. Datta and J. S. Bagla, [arXiv:0908.3857](https://arxiv.org/abs/0908.3857) [astro-ph.CO].
- [21] T. Guha Sarkar, S. Mitra, S. Majumdar and T. R. Choudhury, Mon. Not. Roy. Astron. Soc., **421**, 3570 (2012)
- [22] P. McDonald, Astrophys. J. **585**, 34 (2003).
- [23] R. A. C. Croft, D. H. Weinberg, M. Pettini, L. Hernquist and N. Katz, Astrophys. J. **520**, 1 (1999); R. Mandelbaum, P. McDonald, U. Seljak and R. Cen, Mon. Not. Roy. Astron. Soc. **344**, 776 (2003); M. Viel, S. Matarrese, A. Heavens, M. G. Haehnelt, T. S. Kim, V. Springel and L. Hernquist, Mon. Not. Roy. Astron. Soc. **347**, L26 (2004).
- [24] L. Hui and N. Y. Gnedin, Mon. Not. Roy. Astron. Soc. **292**, 27 (1997); N. Y. Gnedin and L. Hui, Mon. Not. Roy. Astron. Soc. **296**, 44 (1998); P. McDonald, J. Miralda-Escude, M. Rauch, W. L. W. Sargent, T. A. Barlow and R. Cen, Astrophys. J. **562**, 52 (2001) [Erratum-ibid. **598**, 712 (2003)].
- [25] K. M. Lanzetta, A. M. Wolfe and D. A. Turnshek, Astrophys. J., **440**, 435 (1995); L. J. Storrie-Lombardi, R. G. McMahon and M. J. Irwin, Mon. Not. Roy. Astron. Soc., 283, L79 (1996)
- [26] P. McDonald and D. Eisenstein, Phys. Rev. D **76**, 063009 (2007).

- [27] M. McQuinn and M. White, *Mon. Not. Roy. Astron. Soc.* **415**, 2257 (2011).
- [28] A. D. Myers, R. J. Brunner, G. T. Richards, R. C. Nichol, D. P. Schneider and N. A. Bahcall, *Astrophys. J.* **658**, 99 (2007).
- [29] Y. Mao, M. Tegmark, M. McQuinn, M. Zaldarriaga and O. Zahn, *Phys. Rev. D* **78**, 023529 (2008).
- [30] K. K. Datta, S. Bharadwaj and T. R. Choudhury, *Mon. Not. Roy. Astron. Soc.*, **382**, 809 (2007).
- [31] N. Petrovic and S. P. Oh, *Mon. Not. Roy. Astron. Soc.*, **413**, 2103 (2011)
- [32] M. G. Santos, M. B. Silva, J. R. Pritchard, R. Cen and A. Cooray, *Astron. Astrophys.* **527**, A93 (2011).
- [33] D. K. Hazra, M. Aich, R. K. Jain, L. Sriramkumar and T. Souradeep, *JCAP* **1010**, 008 (2010).
- [34] T. Di Matteo, R. Perna, T. Abel and M. J. Rees, *Astrophys. J.* **564**, 576 (2002).
- [35] A. Ghosh, S. Bharadwaj, S. .S. Ali and J. N. Chengalur, *Mon. Not. Roy. Astron. Soc.* **418**, 2584 (2011).
- [36] M. Viel, M. G. Haehnelt and V. Springel, *Mon. Not. Roy. Astron. Soc.* **354**, 684 (2004).